

# Static analysis of thrust bearing with lubrication hole variation in an automobile's connecting rod

Edy Suryono<sup>1,\*</sup>, Gilar Selo Yuda Pratama<sup>2</sup>, Agus Jamaldi<sup>3</sup>

<sup>1,2,3</sup> Sekolah Tinggi Teknologi Warga Surakarta, Indonesia  
E-mail: EDYSURYONO@sttw.ac.id\*

## ABSTRACT

The research used the thrust bearing of a 1298cc automobile. The thrust-bearing material was annealed stainless steel (SS 201) with a tensile strength of 685 MPa and a yield strength of 292 MPa. The research objective was to obtain the best static thrust-bearing analysis results based on CAE software analysis. The research method included design stages, material parameters, fixed geometry determination, loading, meshing settings, computation, and result data. The simulation results were in the form of stress values, where the maximum stress value on the three-hole, one-hole, and non-hole thrust bearings were 227.2 MPa, 215.1 MPa, and 138 MPa, respectively. The non-hole thrust bearing could be the safest among all variations. The non-hole thrust bearing had a critical stress area value of 154 MPa, where it could absorb a force of 52.75% of the yield strength, the lowest strain was  $8.531E-4$ , and had the highest minimum safety factor of 1.896.

This is an open-access article under the CC-BY-SA license.



## ARTICLE INFO

### Article history

Received:  
07 February 2023  
Revised:  
21 March 2023  
Accepted:  
29 March 2023

### Keywords

annealed SS 201  
CAE  
connecting rod  
lubrication hole  
static analysis  
thrust bearing

## 1. Introduction

The engine's connecting rod is a crucial component. It transfers the gas pressure at the top of the piston to the crankshaft, to make it work. The reciprocating inertial force of the piston and the pressure of the piston pin must be supported by the connecting rod [1]–[4]. Thus, it is necessary to analyze the strength of the material. Static analysis using software applications is one of the non-destructive methods of testing materials [5]–[9].

Bearing research to detect defects by focusing on the vibrations generated has been conducted [10], [11]. The variables studied include radial load, axial load, bearing rotational speed, lubrication type, adjustment, and number of rollers [12]–[15]. Meanwhile, to obtain the value of the damage level of the bearing, variations in vibration amplitude are added.

Static analysis research results show that the area where critical stress occurs is located at the radius (fillet) of a part. Theoretically, a part with a small radius will produce greater stress. Where, the smaller the radius, the smaller the surface area. Thus, it will increase the stress that occurs [3], [16], [17].

Connecting rod failure generally occurs due to friction or impact on the connecting rod. Identification of effective and efficient countermeasures against rod metal must be carried out so as not to damage other components [18]. This analysis is needed to determine the ability to withstand excessive pressure on the thrust bearing which has an impact on the occurrence of high stresses so that it reaches the critical value of material strength [19].

Analysis of the rod is required to ensure the longevity of the connecting rod and minimize damage [20]–[22]. Thus, the connecting rod can optimally transmit power from the combustion process to the crankshaft. If during the analysis process, a very high loading occurs on the connecting rod and the thrust bearing is unable to reduce or withstand the explosive force of the combustion process, it is necessary to replace the material or redesign the component [23]–[25].

This study was a static analysis of thrust bearings of a 1298 cc automobile under the forces acting during the combustion process. The main load was piston pressure which was transmitted to the connecting rod and thrust bearing. The thrust bearing material was annealed stainless steel (SS 201). The analysis was carried out to obtain a thrust-bearing design with various lubrication holes with better resistance.

## 2. Method

The research stages included designing parts and assemblies, determining material property values, determining parameters for static analysis, computation, and data analysis. The design stage involved drawing the connecting rod and thrust bearing of a 1298 cc automobile, as shown in Fig. 1.

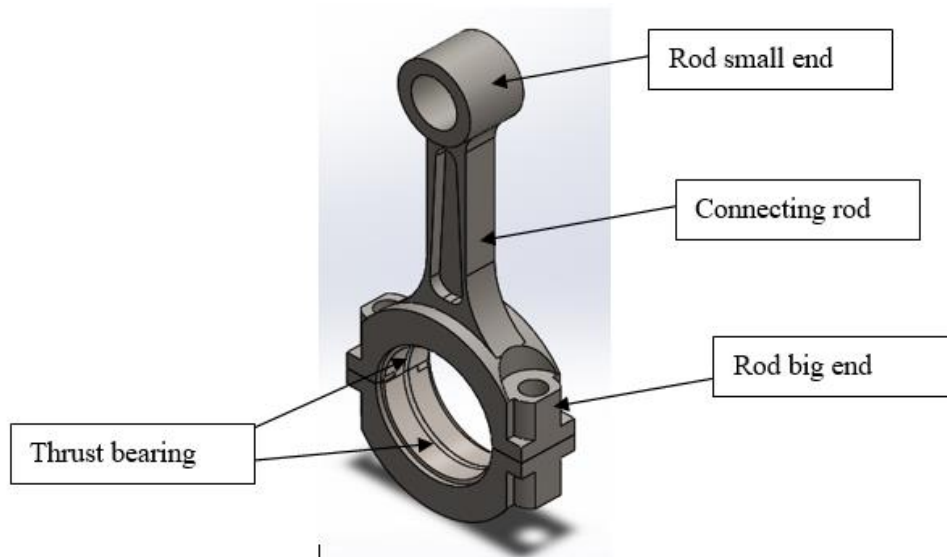


Fig. 1. Connecting rod 3D-design

The design of the various thrust bearing on the automobile can be seen in Fig. 2.



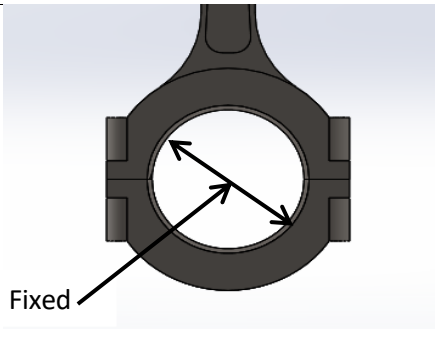
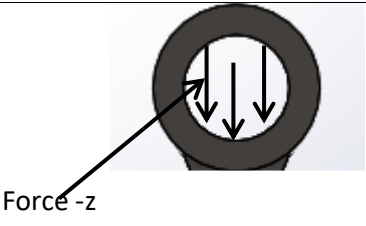
Fig. 2. Various thrust-bearing designs

Table 1 Material properties of the thrust bearing of annealed stainless steel (SS) 201 [1]

Property	Value	Units
Elastic Modulus	207000	N/mm <sup>2</sup>
Poisson's Ratio	0.27	N/A
Tensile Strength	685	MPa
Yield Strength	292	MPa
Thermal Expansion Coefficient	1.7e-005	/K
Mass Density	7860	kg/m <sup>3</sup>
Hardening Factor	0.85	N/A

Table 1 shows the material properties of the thrust bearings. Table 2 shows the placement of the fixed geometry and the loading that was implemented on the connecting rod.

Table 1. Fixture geometry position and loading on the connecting rod

Fixture Name	Fixture image	Fixture Details
Fixed-1		<b>Entities:</b> 4 face(s) <b>Type:</b> Fixed Geometry
Load Name	Load image	Load Details
Force-1		<b>Entities:</b> 1 face(s), 1 plane(s) <b>Reference:</b> Top Plane <b>Type:</b> Apply force <b>Values:</b> ---,---, -4785 N

The next step was to set the mesh size using a curvature-based mesh with a maximum element size of 1.5 mm and a minimum element size of 0.499995 mm, as shown in Table 2. Meanwhile, the meshed connecting rod design can be seen in Fig. 3.

Table 2. Meshing parameters

<i>Mesh Information</i>	<i>Non-hole</i>	<i>One hole</i>	<i>Three-hole</i>
<i>Mesh type</i>	<i>Solid mesh</i>	<i>Solid mesh</i>	<i>Solid mesh</i>
<i>Mesher used</i>	<i>Curvature-based mesh</i>	<i>Curvature-based mesh</i>	<i>Curvature-based mesh</i>
<i>Jacobian points</i>	4 points	4 points	4 points
<i>Max element size</i>	1.5 mm	1.5 mm	1.5 mm
<i>Min element size</i>	0.499995 mm	0.499995 mm	0.499995 mm
<i>Mesh quality</i>	<i>Draft</i>	<i>Draft</i>	<i>Draft</i>
<i>Total nodes</i>	2349	2477	2583
<i>Total elements</i>	8005	8587	8910
<i>Maximum aspect ratio</i>	9.0843	9.0877	8.8047

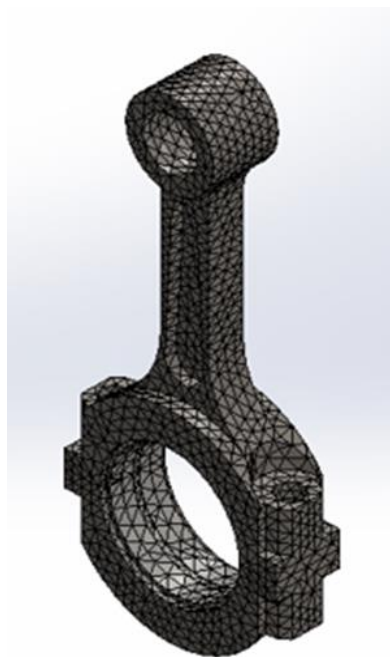


Fig. 3. Meshing of connecting rod and thrust bearing

The simulation comprised simulations of stress, displacement, strain, the factor of safety, and stress in critical areas [26]. The simulation result of the thrust bearing is shown in Fig. 4.

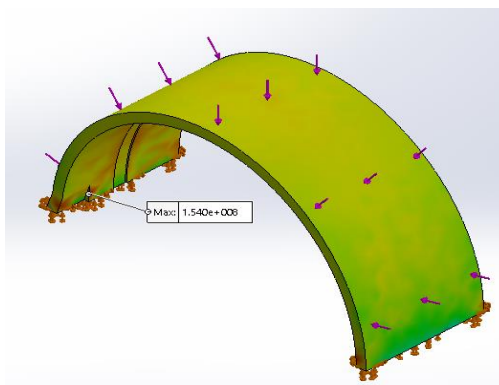


Fig. 4. Static thrust bearing simulation

### 3. Results and Discussion

The research results in the form of stress, displacement, and strain on various thrust-bearing designs are shown in Table 3.

Table 3. Stress, displacement, and strain data on thrust bearings

Design	Stress (MPa)			Displacement (mm)			Strain		
	min	avg	max	min	avg	max	min	avg	max
Non-Hole	52.51	119.9	138.0	1.00E-30	1.475E-2	2.663E-2	1.830E-4	4.864E-4	8.531E-4
One Hole	60.10	120.1	215.1	1.00E-30	1.470E-2	2.581E-2	1.562E-4	4.869E-4	1.069E-3
Three Hole	61.98	121.0	227.2	1.00E-30	1.491E-2	2.710E-2	2.082E-4	4.905E-4	1.276E-3

Meanwhile, the research results in the form of safety factors for various thrust-bearing designs can be seen in Table 4.

Table 4. Safety Factor

Design	Safety Factor		
	MIN	AVG	MAX
<i>Non-Hole</i>	1.896	2.456	6.788
<i>One Hole</i>	1.357	2.459	7.396
<i>Three Hole</i>	1.385	2.448	7.526

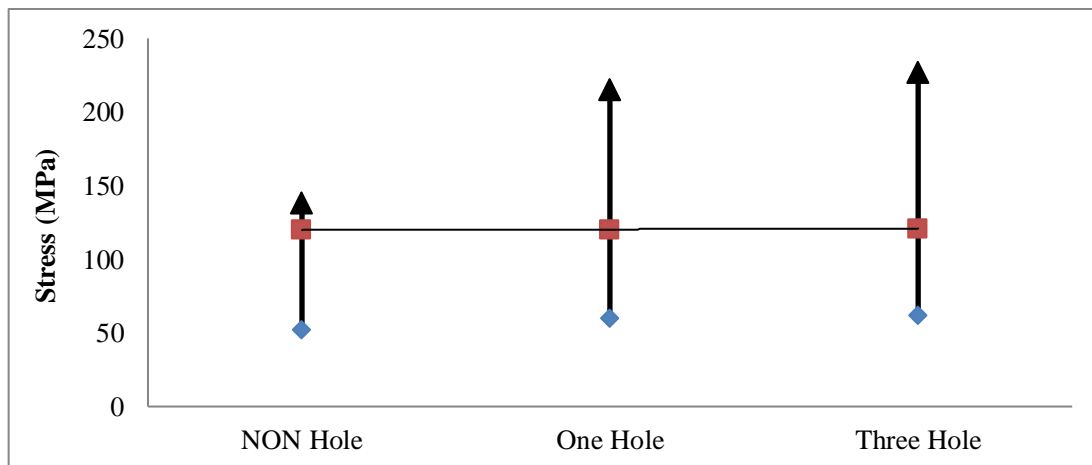


Fig. 5. Thrust-bearing stress

Stresses of various thrust-bearing designs can be seen in Fig. 5. The largest stress value is the one-hole thrust bearing with a value of 215.1 MPa. At the same time, the thrust bearing with the lowest stress is the non-hole thrust bearing with a stress value of 52.51 MPa. Non-hole, one-hole, and three-hole thrust bearings can reduce the force by 52.75%, 26.34%, and 27.81%, respectively. Thus, the greater the percentage reduction in force or stress that occurs due to low loading at yield strength, the safer the material [2], [7]. So non-hole thrust bearing is the safest among other variations.

The displacement values obtained from the three thrust-bearing variations can be seen in Fig. 6. The three-hole thrust bearing has the greatest displacement value of  $2.710E-02$  mm.

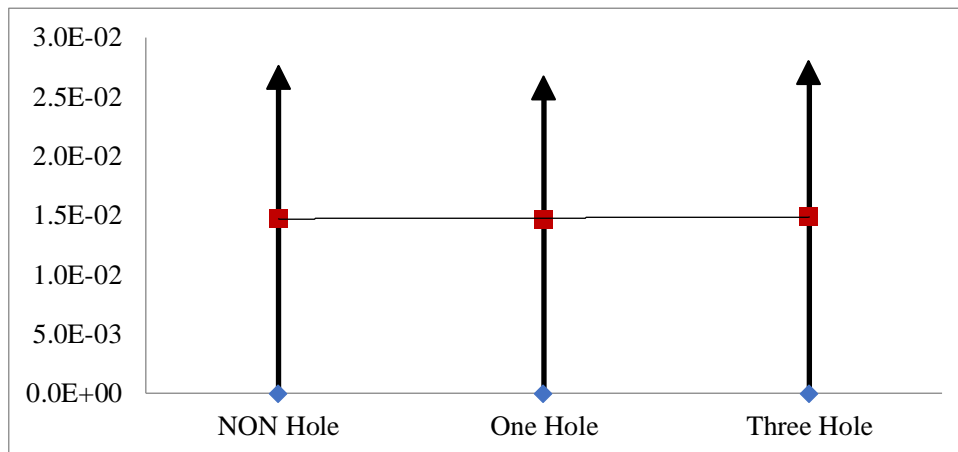


Fig. 6. Thrust-bearing displacement

This proves that the smaller the surface area of the thrust bearing, the more the displacement value will increase [1]. By expanding the cross-sectional area of the connecting rod by 30%, the distortion of the connecting rod's big end bearing was reduced by 4.3%.

The strain values obtained from the three thrust-bearing variations can be seen in Fig. 7. The three-hole thrust bearing has the greatest strain value, namely  $1.276E-03$ ; this made the three-hole thrust bearing experience a large strain.

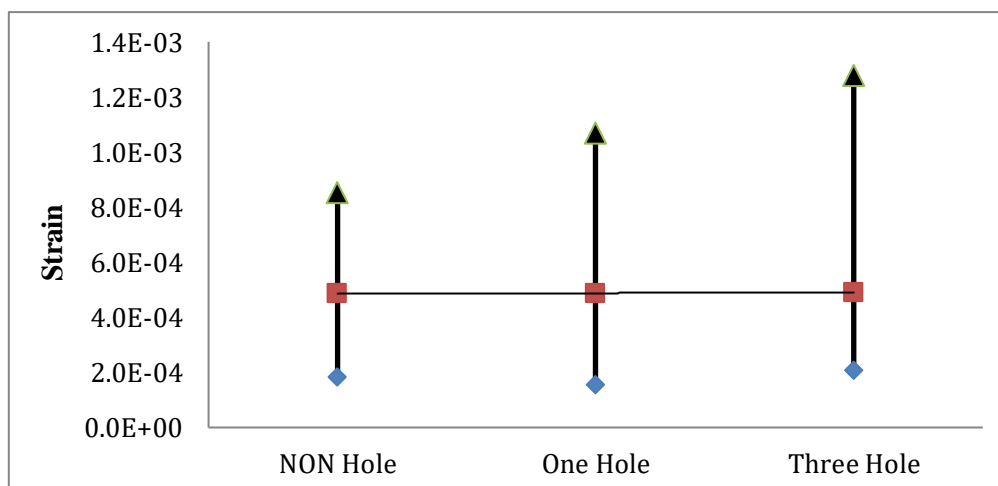


Fig. 7. Thrust-bearing strain

On the other hand, the lowest value is the non-hole thrust bearing with a value of  $8.531E-04$ , which caused the force that could be absorbed by the three-hole thrust bearing smaller than the non-hole thrust bearing.

The results of the safety factor analysis range from 1.357 to 7.526. This is in the range of previous research, where the simulation that has been carried out on the connecting rod produced a safety factor from 1.006 to 15 [4][18]. The safety factor obtained for each specified material can be seen in Fig. 8.

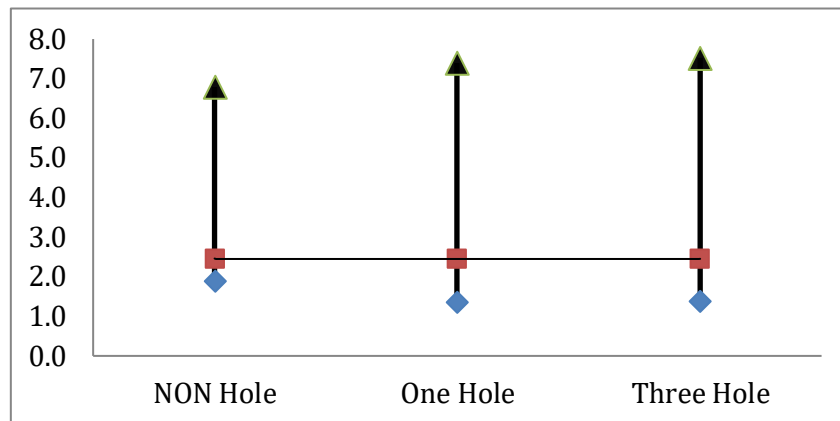


Fig. 8. Safety factor of various thrust-bearing designs

Fig. 8 shows that the greatest safety factor is achieved by the three-hole thrust bearing of 7.526, but with a minimum value of a safety factor of 1.385. This value is lower than the minimum value of the non-hole thrust-bearing safety factor of 1.896. So, the non-hole thrust bearing is relatively the safest among other variations of the thrust bearing.

The critical area in the thrust bearing analysis occurred on the side of the lubrication hole, as shown in Fig. 9. The maximum stress that occurs is 227.2 MPa. Compared to the yield strength of the material, the material experienced a stress of 77.81% or a safety factor of 1.285. The safety factor is still safe because the value is greater than 1 [7], [26], [27].

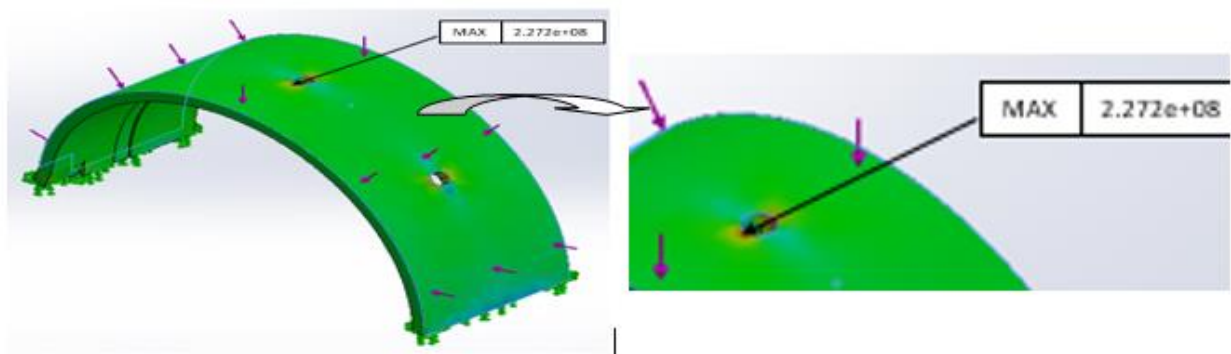


Fig. 9. The critical area that occurs in the thrust-bearing

The maximum stress resulting from the critical area analysis for each variation of thrust-bearing can be seen in Fig. 10. It shows the maximum stress of the largest critical area of the three-hole thrust bearing of 227.2 MPa and the smallest critical area maximum stress of the non-hole thrust bearing of 154.0 MPa.

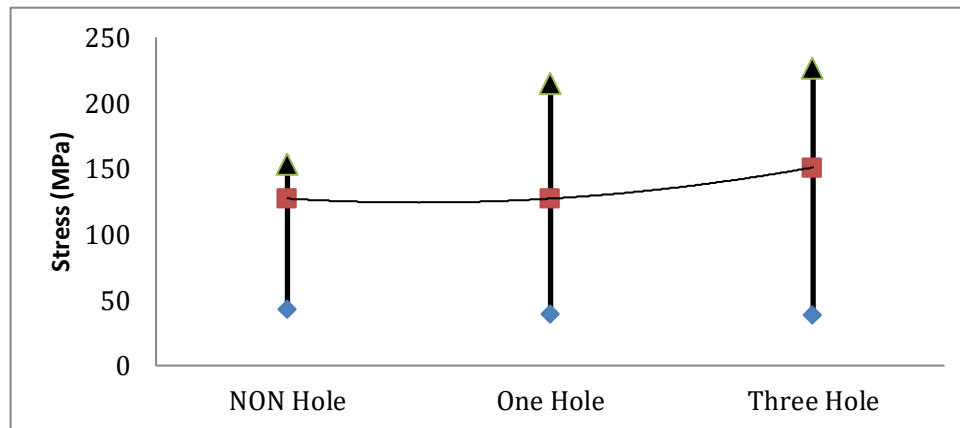


Fig. 10. Critical area stress of thrust bearing

The highest effect of loading occurred in the three-hole thrust bearing, which is equal to 77.81%. However, this is still below the yield strength limit of the material. So, it can be concluded that the material is still safe in critical areas.

#### 4. Conclusion

Based on the results of the study it can be concluded that thrust bearings with non-hole could be the safest thrust bearing compared to the one-hole and three-hole variations. Non-hole thrust bearing had a critical stress area value of  $1.540E+08$  where it could absorb a force of 52.75% of the yield strength, the lowest strain was  $8.531e-4$ , and the highest minimum safety factor of 1.896.

#### References

- [1] P. Zhang, Z. Liu, T. Jin, W. Chen, Y. Zhu, and Z. Zheng, "Design and analysis of five-link-rod rigid constraint support scheme for engine-accessory system vibration control," *Adv. Mech. Eng.*, vol. 11, no. 10, pp. 1–10, 2019, doi: 10.1177/1687814019881281.
- [2] L. Witek and P. Zelek, "Stress and failure analysis of the connecting rod of diesel engine," *Eng. Fail. Anal.*, vol. 97, no. December 2018, pp. 374–382, 2019, doi: 10.1016/j.engfailanal.2019.01.004.
- [3] J. C. Zhu, H. H. Zhu, S. D. Fan, L. J. Xue, and Y. F. Li, "A study on the influence of oil film lubrication to the strength of engine connecting rod components," *Eng. Fail. Anal.*, vol. 63, pp. 94–105, 2016, doi: 10.1016/j.engfailanal.2016.02.006.
- [4] Z. Pan and Y. Zhang, "Numerical investigation into high cycle fatigue of aero kerosene piston engine connecting rod," *Eng. Fail. Anal.*, vol. 120, no. October 2020, p. 105028, 2021, doi: 10.1016/j.engfailanal.2020.105028.
- [5] A. Affandi and S. Huzni, "Analisis Numerik Kekuatan Puntir Baja Karbon Rendah Menggunakan Software (Solidworks)," *R.E.M. (Rekayasa Energi Manufaktur)*, vol. 6, no. 2, pp. 29–36, 2021.
- [6] I. Tanjung, Affandi, and A. R. Nasution, "Analisis Numerik Kekuatan Tarik Plat Baja Karbon Rendah Yang Disambung Dengan Pengelasan Menggunakan Software Solidworks," *R.E.M. (Rekayasa Energi Manufaktur)*, vol. 7, no. 1, pp. 7–14, 2022.

- [7] M. S. D. Ellianto and Y. E. Nurcahyo, "Rancang Bangun dan Simulasi Pembebanan Statik pada Sasis Mobil Hemat Energi Kategori Prototype," *J. Engine Energi, Manufaktur, dan Mater.*, vol. 4, no. 2, pp. 53–58, 2020.
- [8] R. Hapidansyah, "Analisis Simulasi Statik Poros Generator 500 Watt Menggunakan Material Aisi 1020 Dan Aluminium Alloy 6061," *Al Jazari J. Ilm. Tek. Mesin*, vol. 7, no. 2, pp. 65–71, 2022, doi: 10.31602/al-jazari.v7i2.8627.
- [9] L. A. N. Wibawa and T. Tuswan, "Simulasi numerik kekuatan rak roket portabel menggunakan metode elemen hingga," *J. Tek. Mesin Indones.*, vol. 16, no. 2, pp. 54–59, 2021, [Online]. Available: <http://jurnal.bkstm.org/index.php/jtmi/article/view/242>.
- [10] I. M. Jamadar and D. P. Vakharia, "A novel approach integrating dimensional analysis and neural networks for the detection of localized faults in roller bearings," *Meas. J. Int. Meas. Confed.*, vol. 94, pp. 177–185, 2016, doi: 10.1016/j.measurement.2016.07.086.
- [11] M. Tiwari, K. Gupta, and O. Prakash, "Effect of radial internal clearance of a ball bearing on the dynamics of a balanced horizontal rotor," *J. Sound Vib.*, vol. 238, no. 5, pp. 723–756, 2000, doi: 10.1006/jsvi.1999.3109.
- [12] Y. Zhuo, X. Zhou, and C. Yang, "Dynamic analysis of double-row self-aligning ball bearings due to applied loads, internal clearance, surface waviness and number of balls," *J. Sound Vib.*, vol. 333, no. 23, pp. 6170–6189, 2014, doi: 10.1016/j.jsv.2014.04.054.
- [13] C. Bai, H. Zhang, and Q. Xu, "Effects of axial preload of ball bearing on the nonlinear dynamic characteristics of a rotor-bearing system," *Nonlinear Dyn.*, vol. 53, no. 3, pp. 173–190, 2008, doi: 10.1007/s11071-007-9306-2.
- [14] D. Jia *et al.*, "Research on optimizing the axial force of thread connection of engine connecting rod," *Eng. Fail. Anal.*, vol. 130, no. June, p. 105771, 2021, doi: 10.1016/j.engfailanal.2021.105771.
- [15] Z. He *et al.*, "Tribological performances of connecting rod and by using orthogonal experiment, regression method and response surface methodology," *Appl. Soft Comput. J.*, vol. 29, pp. 436–449, 2015, doi: 10.1016/j.asoc.2015.01.009.
- [16] Achmad Zainuri, "Tegangan Maksimum Dan Faktor Keamanan Pada Poros Engkol Daihatsu Zebra Espass Berdasarkan Metode Numerik," *Momentum*, vol. 6, no. 2, pp. 42–47, 2010, [Online]. Available: <http://www.capellagroup.com/cm/sp>.
- [17] E. Suryono, N. W. Darmaatmadja, and B. Margono, "OPTIMASI ALUR PASAK DENGAN VARIASI FILLET DAN CHAMFER UNTUK MENINGKATKAN KEKUATAN POROS AISI 1045," *J. Media Mesin*, vol. 22, no. 2, pp. 118–128, 2021.
- [18] H. M. M. Ali and M. Haneef, "Analysis of Fatigue Stresses on Connecting Rod Subjected to Concentrated Loads At The Big End," *Mater. Today Proc.*, vol. 2, no. 4–5, pp. 2094–2103, 2015, doi: 10.1016/j.matpr.2015.07.205.
- [19] F. E. Kembara, "Analisis Kerusakan Metal Jalan Pada Motor Diesel Generator Di Mv. Energy Prosperity," pp. 1–45, 2019, [Online]. Available: [http://repository.pip-semarang.ac.id/id/eprint/1900%0Ahttp://repository.pip-semarang.ac.id/1900/2/52155713T\\_SKRIPSI\\_OPEN\\_ACCESS.pdf](http://repository.pip-semarang.ac.id/id/eprint/1900%0Ahttp://repository.pip-semarang.ac.id/1900/2/52155713T_SKRIPSI_OPEN_ACCESS.pdf).
- [20] S. Rakic, U. Bugaric, I. Radisavljevic, and Z. Bulatovic, "Failure analysis of a special vehicle engine connecting rod," *Eng. Fail. Anal.*, vol. 79, no. August 2016, pp. 98–109, 2017, doi: 10.1016/j.engfailanal.2017.04.014.
- [21] J. H. Son, S. C. Ahn, J. G. Bae, and M. Y. Ha, "Fretting damage prediction of connecting rod of marine diesel engine," *J. Mech. Sci. Technol.*, vol. 25, no. 2, pp. 441–447, 2011, doi:

- 10.1007/s12206-010-1206-6.
- [22] A. R. Pani, R. K. Patel, and G. K. Ghosh, "Buckling analysis and material selection of connecting rod to avoid hydro-lock failure," *Mater. Today Proc.*, vol. 27, pp. 2121–2126, 2019, doi: 10.1016/j.matpr.2019.09.079.
- [23] D. T. Y. Tatang and D. N. Adnyana, "Analisa Kegagalan Conrod Bearing Pada Kapal Cepat," *J. Teknol. dan Rekayasa Manufaktur*, vol. 3, no. 2, pp. 87–98, 2021, doi: 10.48182/jtrm.v3i2.82.
- [24] H. Ramadhan, S. Nugroho, and M. Tauviquirrahman, "Analisis Kegagalan Pada Komponen Connecting Rod Mobil Kapasitas 1300 Cc," *J. Tek. Mesin S-1*, vol. 9, no. 3, pp. 375–380, 2022.
- [25] K. Khaeroman and W. A. Putranto, "Studi Kasus Analisis Kegagalan Baut Connecting Rod Mesin Diesel Generator Kapal," *Inovtek Polbeng*, vol. 11, no. 1, pp. 49–54, 2021, [Online]. Available: <http://ejournal.polbeng.ac.id/index.php/IP/article/view/1749>.
- [26] S. Suryady and E. A. Nugroho, "Simulasi Faktor Keamanan Dan Pembebanan Statik Rangka Pada Turbin Angin Savonius," *J. Ilm. Multidisiplin*, vol. 1, no. 2, pp. 42–48, 2022.
- [27] Z. Abidin and B. R. Rama, "Analisa Distribusi Tegangan Dan Defleksi Connecting Rod Sepeda Motor 100 Cc Menggunakan Metode Elemen Hingga," *J. Rekayasa Mesin*, vol. 15, no. 1, pp. 30–39, 2015.